nature materials

Supplementary information

https://doi.org/10.1038/s41563-024-02037-1

Human immune organoids to decode B cell response in healthy donors and patients with lymphoma

In the format provided by the authors and unedited

Supplementary Information

Supplementary Figure 1	Characterization of human tonsil tissues.
Supplementary Figure 2	Bioengineered PEG-4MAL hydrogel-based tonsil organoids.
Supplementary Figure 3	PEG-4MAL hydrogel-based PBMC organoids.
Supplementary Figure 4	B cell subtypes in PEG-4MAL hydrogel-based immune organoids.
Supplementary Figure 5	Follicular Helper T cells in bioengineered PEG-4MAL hydrogel-based PBMC organoids.
Supplementary Figure 6	B cells from tonsil mononuclear cells compared to those from PBMCs at day 0.
Supplementary Figure 7	Bioengineered PEG-4MAL hydrogel-based immune organoids.
Supplementary Figure 8	H1N1-specific ELISPOT for PBMC-derived and tonsil-derived 2D co- cultures.
Supplementary Figure 9	tSNE plots of LZ and DZ distribution over 24 days.
Supplementary Figure 10	Response to Fluzone vaccine.

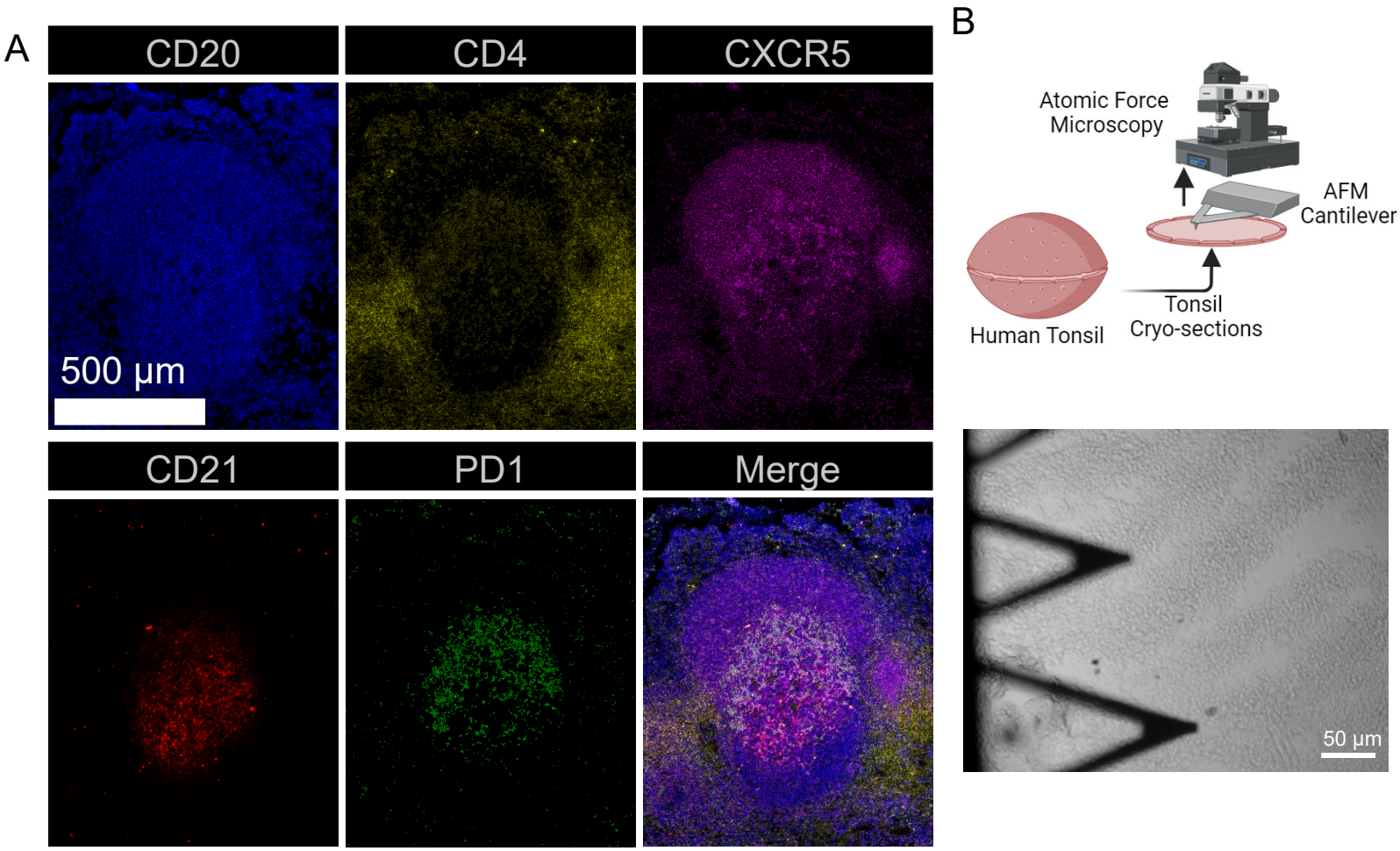

Supplementary Figure 1: Characterization of human tonsil tissues.

A) Immunofluorescence of human tonsil tissues demonstrating the spatial organization of B cells (CD20), T cells (CD4), follicular helper T cells (CD4, CXCR5, PD1), and follicular dendritic cells (CD21). Representative images of results from 3 donors.

B) (Top)Workflow for assessing the stiffness of tonsil tissues utilizing Atomic Force Microscopy (AFM) includes the preparation and cryo-sections generation of the tissue samples, calibration of the AFM instrument with an appropriate probe, precise force application and indentation measurements with the AFM tip. (Bottom) Region of interest of tonsil tissue cryosection in a representative section as visualized by the AFM-mounted light microscope. The AFM cantilever is shown above the tissue.

Supplementary Figure 2, Related to Figure 2

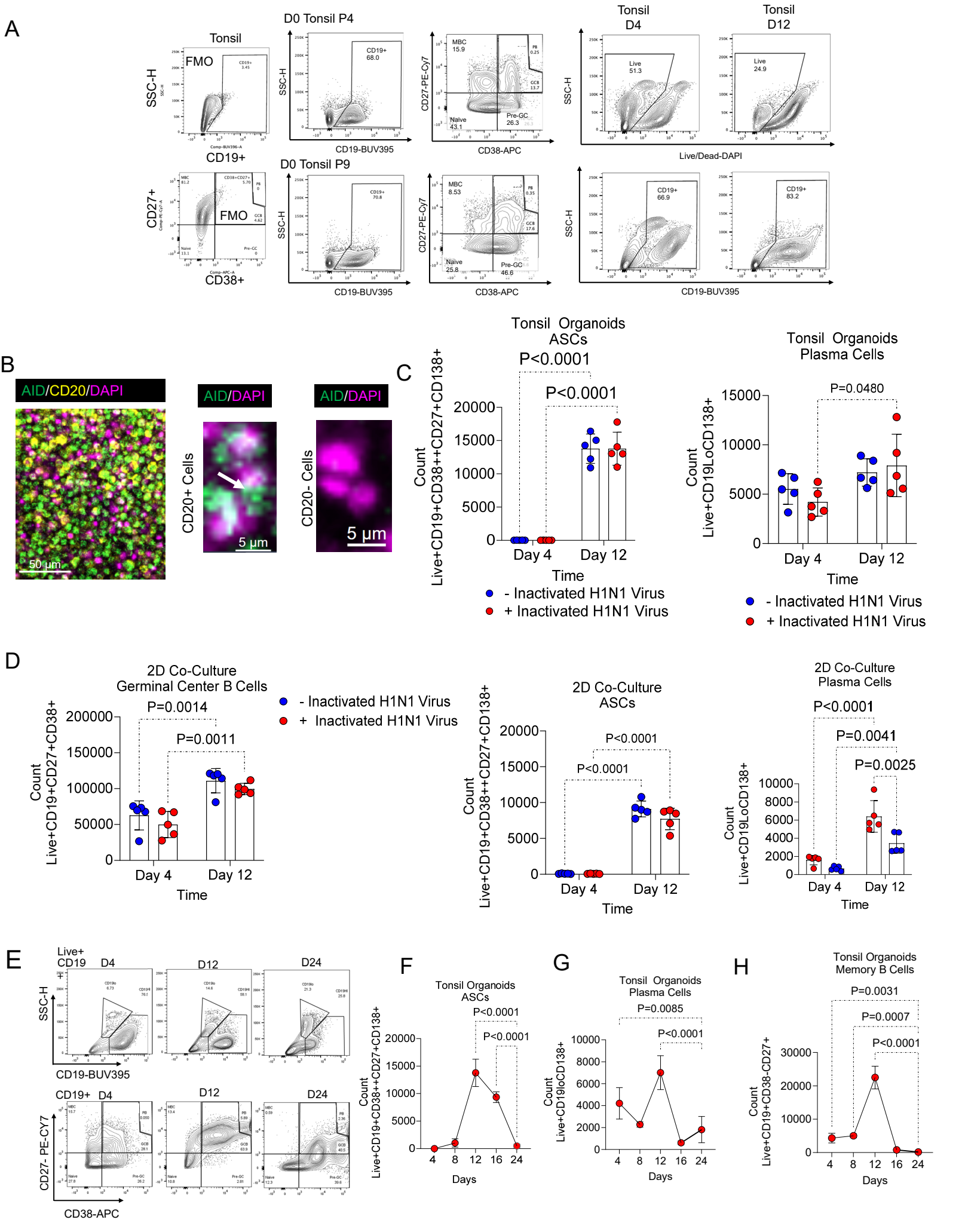

Supplementary Figure 2: Bioengineered PEG-4MAL hydrogel-based tonsil organoids.

A) Representative flow cytometry gating of tonsil cells in organoids on days 0, 4, and 12 of culture across two tonsil donors (#4 and #9).

B) Immunofluorescence staining with AID protein (green) in PBMC organoids on D12. Arrows represent areas with or without AID. Experiment was repeated 3 times with similar results.

C) The count of ASCs and plasma cells on D4 and D12 in response to antigen (inactivated H1N1 virus) stimulation in tonsil organoids (Mean ± S.D; N = 5 technical replicates from a donor). Two-way ANOVA with Tukey's posthoc test.

D) The count of B cell phenotypes (GC B cells, ASCs, PCs) on D4 and D12 in response to antigen (inactivated H1N1 virus) stimulation in 2D tonsil, CD40L-TCM, HK-FDCs co-culture. (Mean ± S.D; N = 5 technical replicates from a donor). Two-way ANOVA with Tukey's posthoc test.

E) Representative flow cytometry gating of B cell phenotypes in tonsil organoids over 24 days.

F-H) The counts of ASC (F), plasma cells (G), and memory B cells (H) over 24-day tonsil organoids culture. Mean ± S.D. One-way ANOVA posthoc test. Each dot represents an average of 5 technical replicates from the same donor.

Supplementary Figure 3, Related to Figure 2

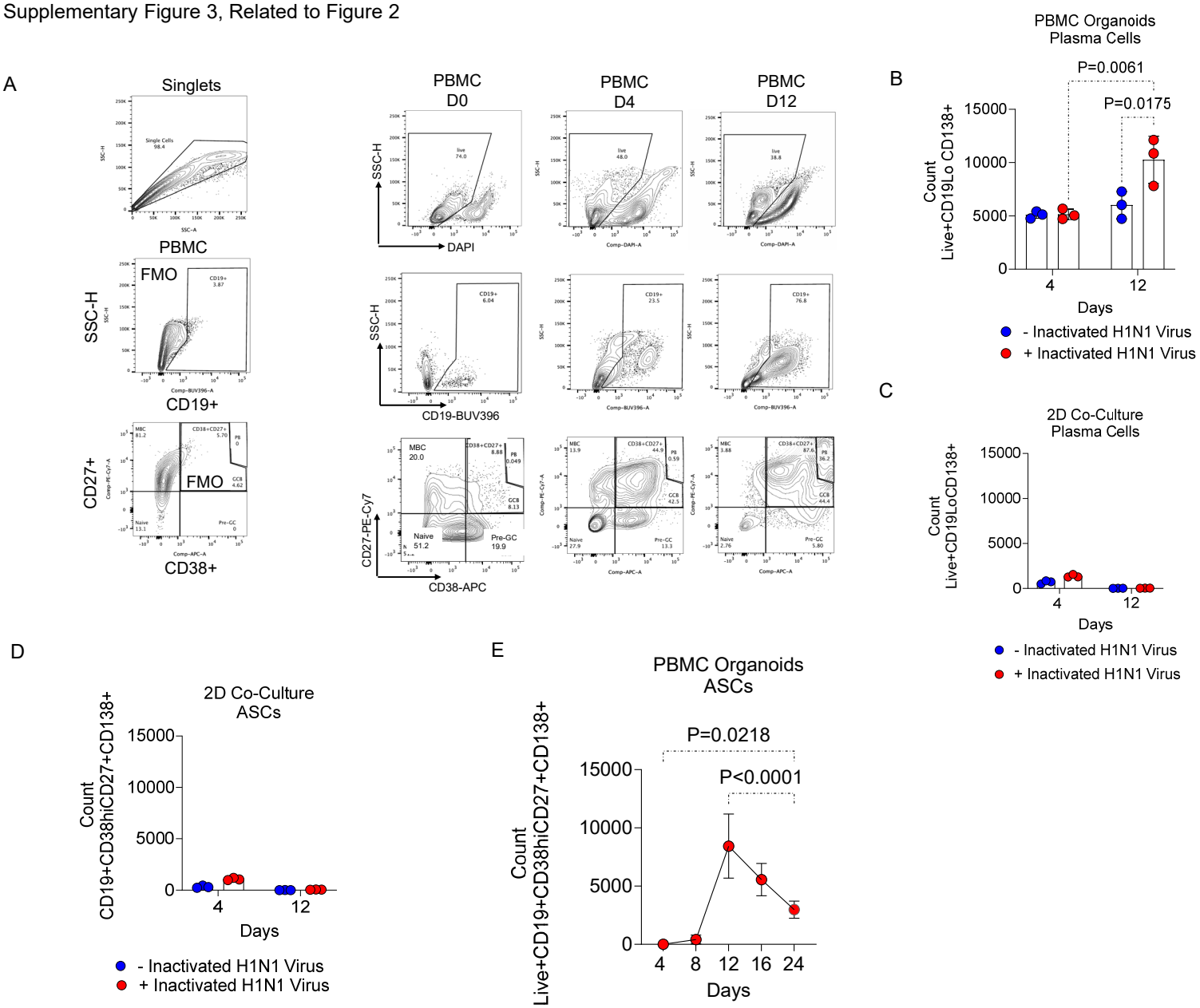

Supplementary Figure 3: PEG-4MAL hydrogel-based PBMC organoids.

A) Representative flow cytometry gating of B cells from PBMC-derived organoids over 12 days of culture.

B-C) Count of plasma cells on D4 and D12 in response to antigen (inactivated H1N1 virus) stimulation in PBMC organoids (B) and in 2D co-cultured with CD40L-TCM and HK-FDCs (C) (Mean ± S.D; N = 3 technical replicates from a donor). Two-way ANOVA with Tukey's post-hoc test.

D) Count of ASCs on D4 and D12 in response to antigen (inactivated H1N1 virus) stimulation in 2D PBMC, CD40L-TCM, HK-FDCs co-culture. (Mean ± S.D; N = 3 technical replicates from a donor). Two-way ANOVA with Tukey's post-hoc test.

E) Counts of ASCs over 24-day PBMC organoids culture. Mean ± S.D. One-way ANOVA posthoc test. Each dot represents an average of 4-5 organoid technical replicates from the same donor.

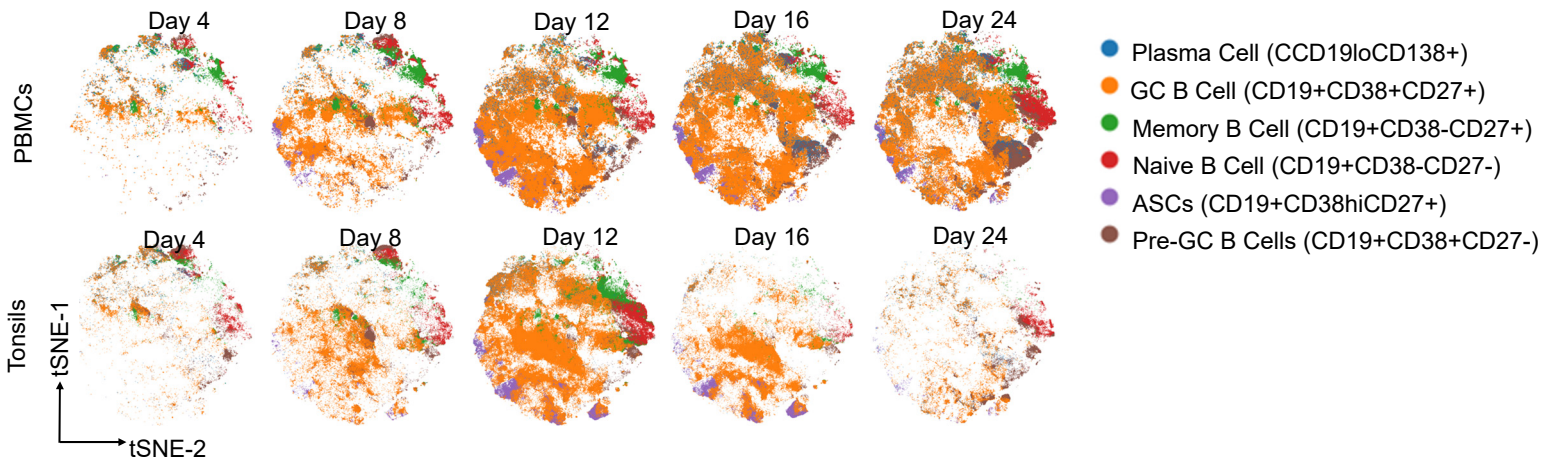

Supplementary Figure 4: B cell subtypes in PEG-4MAL hydrogel-based immune organoids. tSNE plots of B cell subtypes in tonsil organoids vs PBMC organoids over 24 days. Data were extracted as single cells from flow cytometry.

Supplementary Figure 5, Related to Figure 2

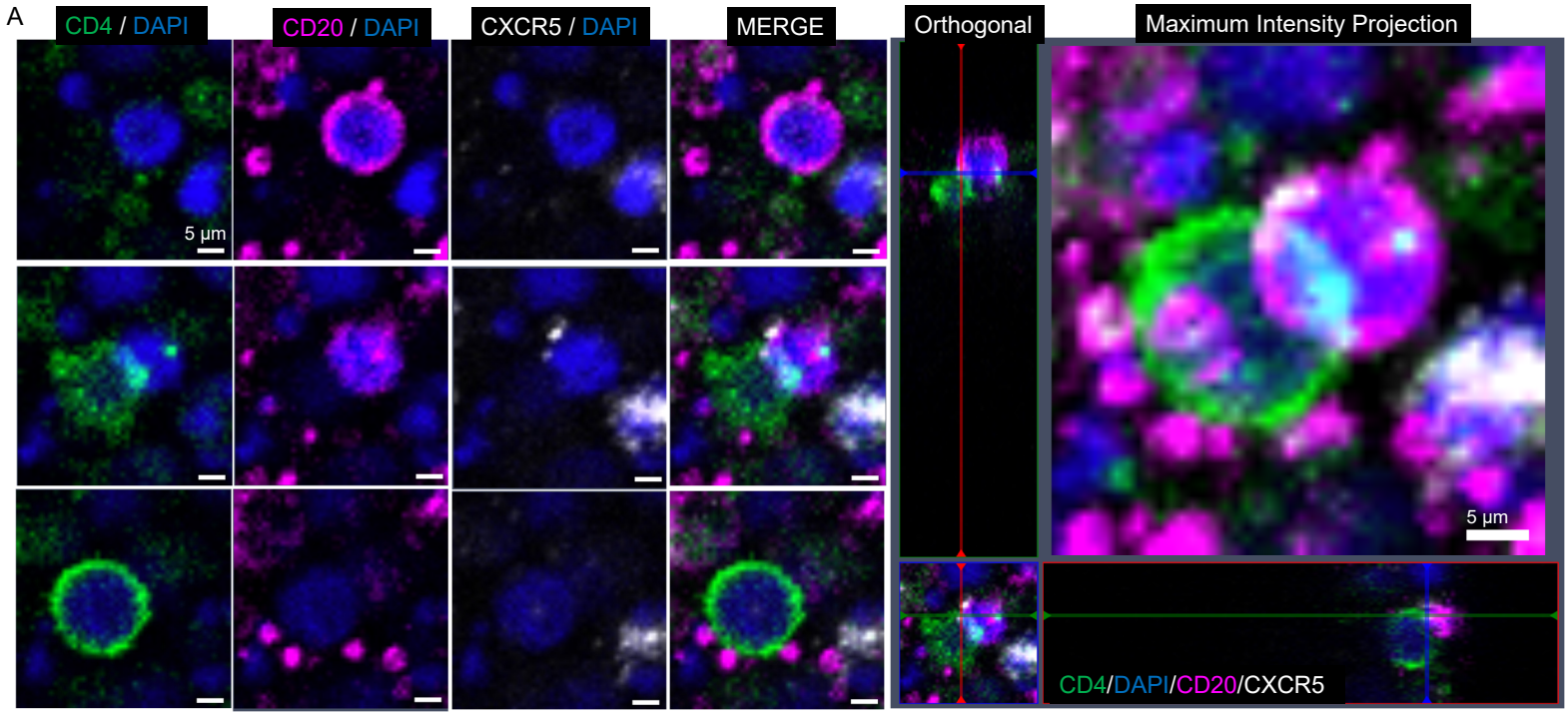

Supplementary Figure 5: Follicular Helper T cells in bioengineered PEG-4MAL hydrogel-based PBMC organoids. Immunofluorescence staining captured the interaction of B cell (pink), CD4 T cell (green), and follicular helper T cell (green, white). Experiment was repeated 3 times with similar results.

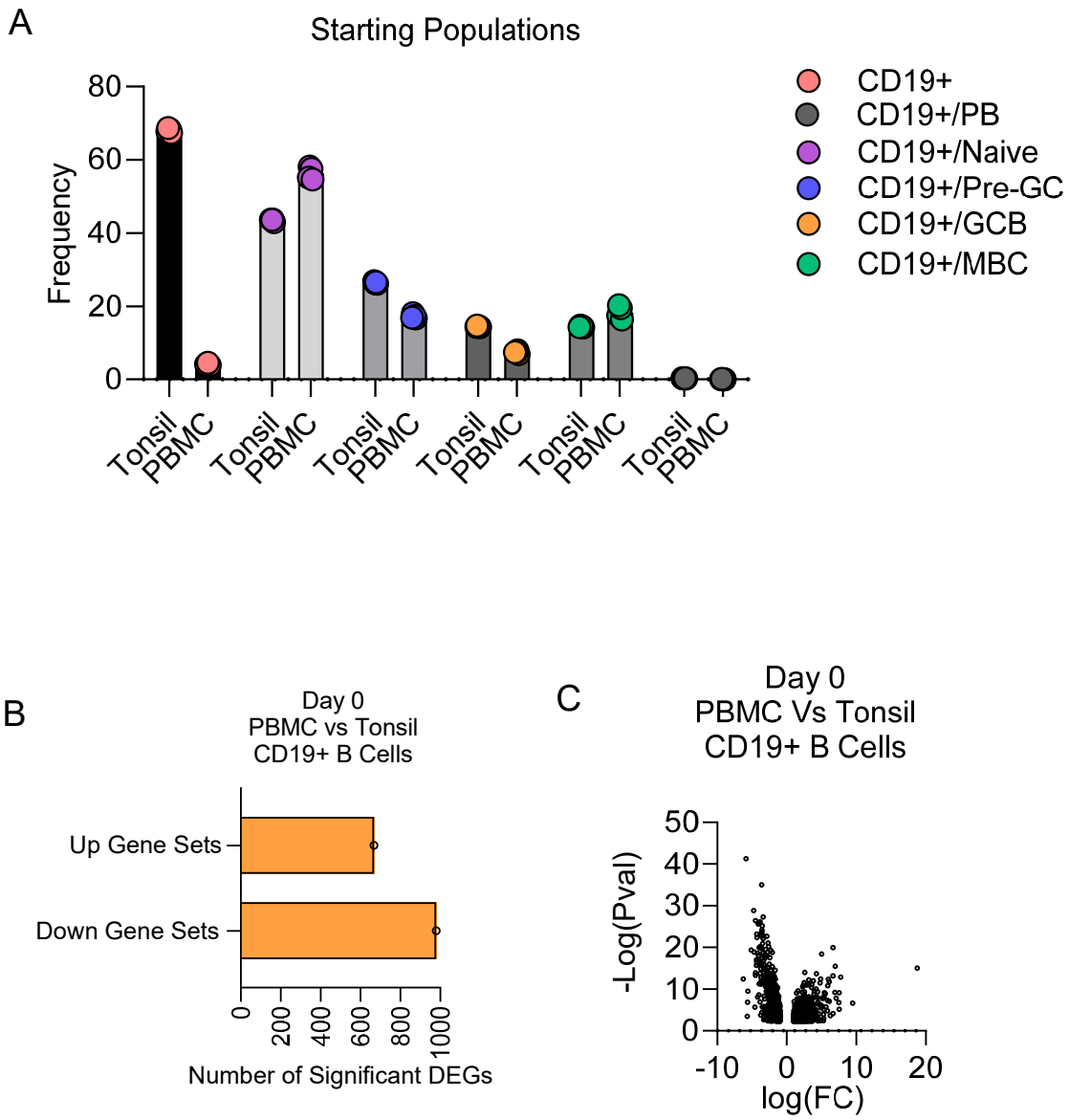

Supplementary Figure 6: B cells from tonsil mononuclear cells compared to those from PBMCs at day 0.

A) Percentage of Starting B cell phenotypes in tonsil mononuclear cells and PBMCs on D0.

B) Bulk RNA-seq analysis of CD19+ B cells without treatment from 3-donor tonsils (P4, P7, P10) and 3- donor PBMCs (802C, 811C, 902C) on D0.

C) A volcano plot provides a visual representation of significant gene expression differences derived from bulk RNA sequencing of CD19+ B cells, comparing samples from the tonsils of 3 donors to PBMCs from a separate set of 3 donors, all collected on D0.

Supplementary Figure 7, Related to Figure 2

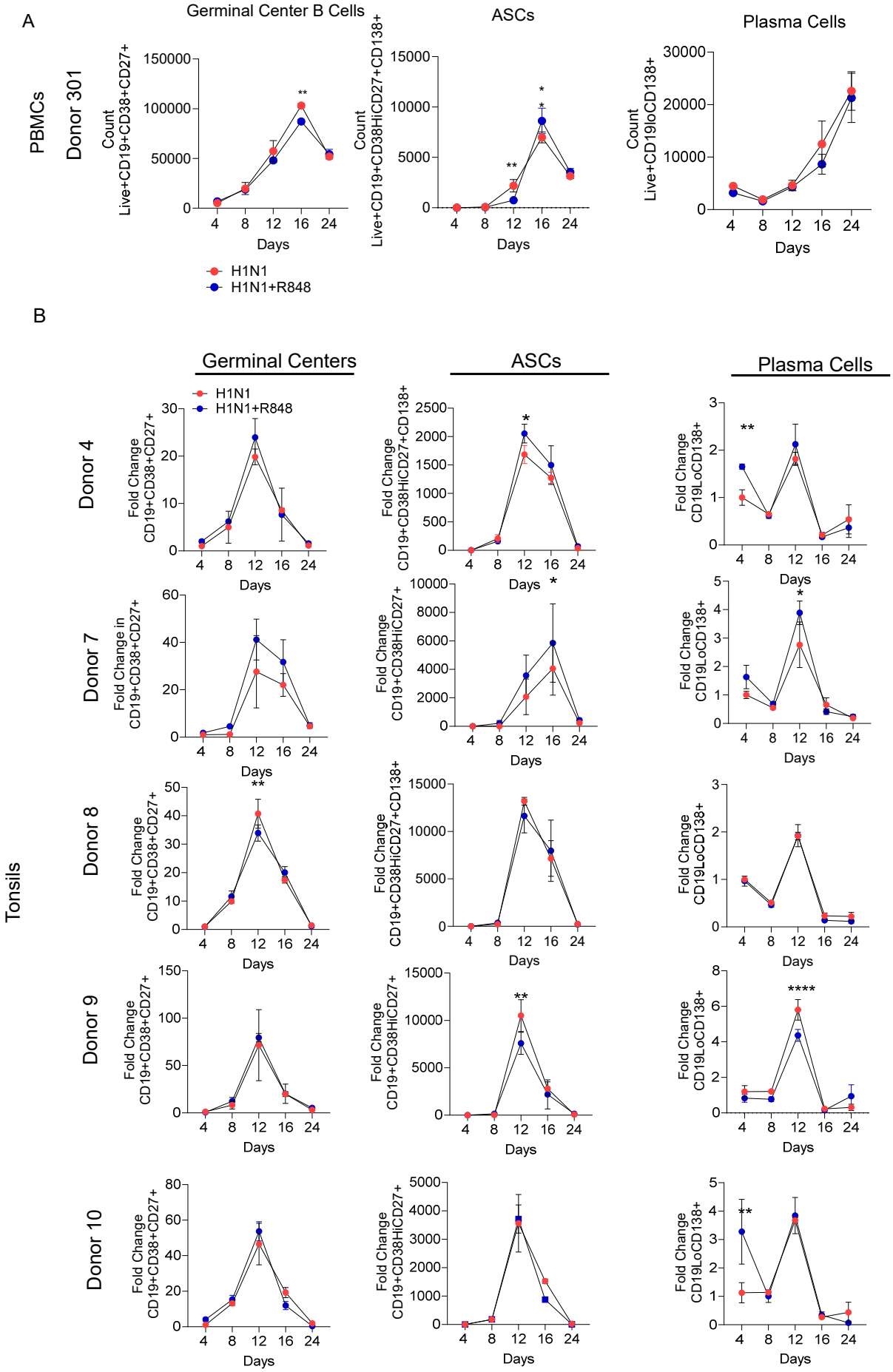

Supplementary Figure 7: Bioengineered PEG-4MAL hydrogel-based immune organoids.

A) Count of GC B cells, ASCs, and plasma cells over 24 days of PBMC organoids, from donor 301, when incubated with antigen (inactivated H1N1 virus) and antigen with TLR7/8 agonist R848. Mean ± S.D. One-way ANOVA with Sidak's multiple comparison test. Each dot represents an average of 3 organoid technical replicates from the same donor. *P < 0.05; **P < 0.01;***P < 0.001; ****P < 0.0001.

B) Fold change of GC B cells, ASCs, and plasma cells over 24 days of tonsil organoids, from 5 donors, when incubated with antigen (inactivated H1N1 virus) and antigen with TLR7/8 agonist R848. Mean ± S.D. One-way ANOVA with Sidak's multiple comparison test. Each dot represents an average of 3 organoid technical replicates from the same donor. *P < 0.05; **P < 0.01;***P< 0.001; ****P < 0.0001.

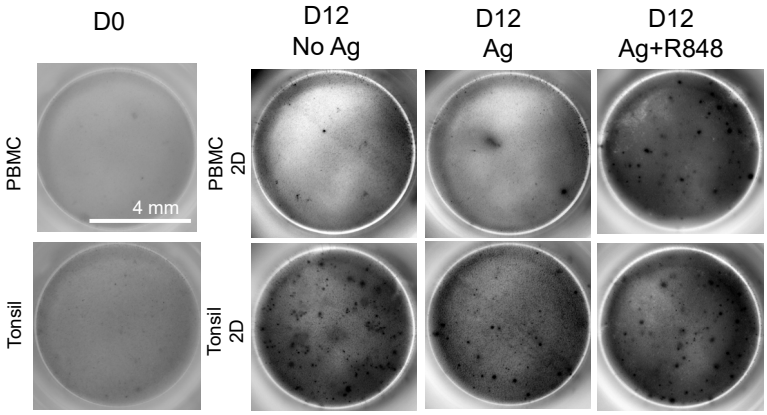

Supplementary Figure 8: H1N1-specific ELISPOT for PBMC-derived and tonsil-derived 2D co- cultures. Brightfield images of H1N1-specific ELISPOT for PBMC-derived and tonsil-derived 2D co- culture with CD40L-TCM and HK-FDCs on D0 and D12 with control, inactivated H1N1 virus alone, and inactivated H1N1 with R848.

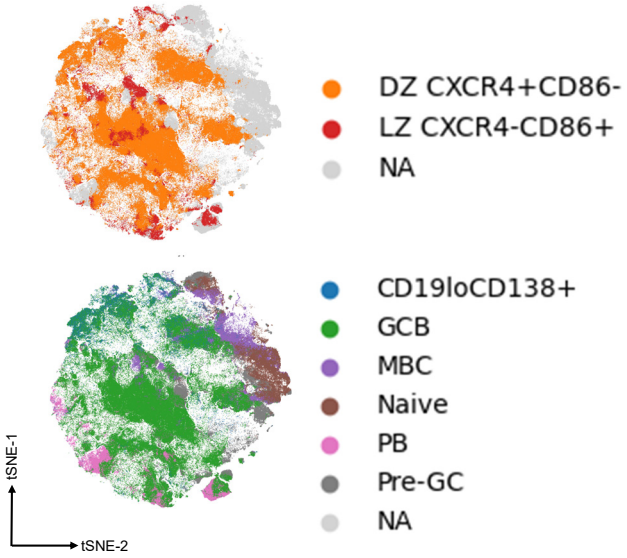

Supplementary Figure 9: tSNE plots of LZ and DZ distribution relative to distinct B cell phenotypes in PBMC organoids over 24 days. Data were extracted as single cells from flow cytometry.

Supplementary Figure 10, Related to Fig 5

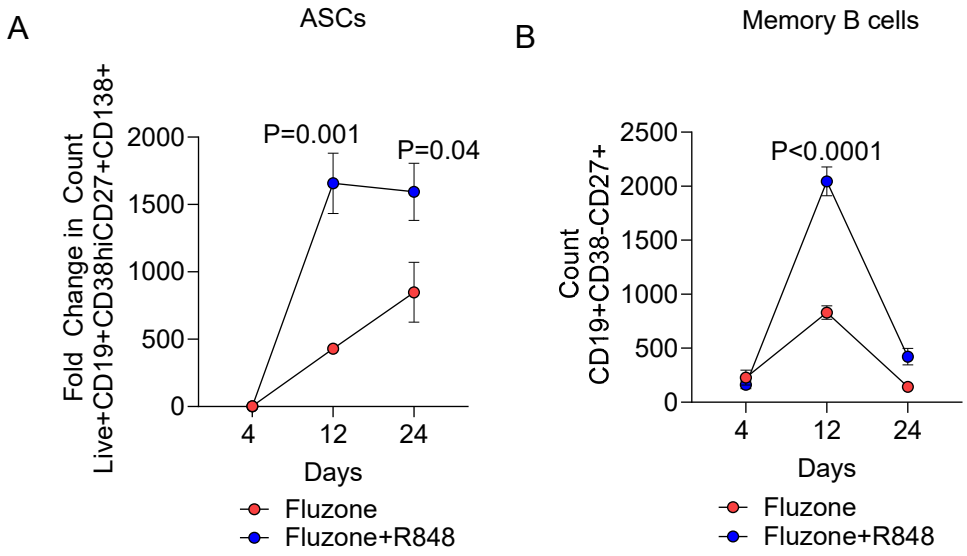

Supplementary Figure 10: Response to Fluzone vaccine. A-B) Fold change in the count of ASCs (A) and memory B cells (B) over 24-day PBMC-derived organoid culture from a healthy donor following the treatment of Fluzone vaccine or the co-treatment of Fluzone vaccine and R848. Mean ± S.D. Two-way ANOVA with Tukey's posthoc test. Each dot represents an average of 3 technical replicates from the same donor. For all $P < 0.0001$, $P = 0.00001$.